On the process of rotational augmentation

On the process of Rotational Augmentation

Wolf-Gerrit Früh
School of Engineering and Physical Sciences,
Heriot Watt University, Riccarton, Edinburgh EH14 4AS, UK
email: w.g.fruh@hw.ac.uk

March 28, 2008

Abstract

Rotational augmentation is a well-known phenomenon of rotating aerofoils as found for wind turbines and helicopters, by which the lift or torque is improved compared to lift coefficient measurements of the same stationary aerofoil.

We present an analysis which is based on the concept of a developing boundary layer and the Ekman boundary layer in a rotating fluid. The work uses a 3D Finite-Element Analysis of the developing boundary layer over a flat plate in a rotating frame of reference, where the Reynolds number, the Ekman number, and the speed ratio, were varied as the three main parameters of the system.

The results demonstrates that the primary effect of rotation is to induce a span-wise flow in the radial direction which in turn leads to mass transport into the developing boundary layer from above by a process known as Ekman suction. This Ekman suction then results in a reduction of the boundary layer growth compared to the standard, no-rotating boundary layer.

1 Introduction

Rotational augmentation is a well-known phenomenon of rotating aerofoils as found for wind turbines and helicopters, by which the lift or torque is improved compared to lift coefficient measurements of the same stationary aerofoil. Besides the result of improved lift, the main characteristic in the velocity fields is a noticeable cross flow within the boundary layer radially outwards.

An order-of-magnitude analysis has shown that the Coriolis acceleration can reduce adverse pressure gradients and, with it, the onset of stall [7, 3] and some experiments have suggested that a spanwise variation of the boundary layer development on a rotating blade can lead to conditions in which the onset of ow separation is delayed to a higher angle of attack. Overall, however, a rigorous analysis and understanding is still lacking [4]. A boundary-layer analysis suggested that the growth of the boundary layer would be limited to about nine to ten times the Ekman layer thickness [2].

While other recent studies, [6], have used advanced CFD tools to investigate this problem in its full complexity of a three-dimensional, rotating turbine blade, we aim to contribute to this problem by reducing the system to a minimum complexity. To this end, we consider only the most basic developing boundary layer and investigate its response to added Coriolis and centrifugal forcing.

Since the resulting flow is intrinsically three-dimensional, with the vertical variation of the mean flow and the induced cross-flow, the analysis discussed here is based on a 3D Finite-Element model of laminar flow over a flat plate in a rotating frame of reference, where the rotational axis is perpendicular to the plate's surface. This model was used for a series of parametric studies for the main three nondimensional parameters, the Reynolds number, the Ekman number, and the speed ratio. These paramters and the basic theory is summarised in the following sub-section. The model set-up and the modelling methodology are described in section 2, followed by the presentation of the results. Section 4 concludes the paper with some conclusions.

1.1 Blasius and Ekman boundary layers

The basic momentum equation for an incompressible Newtonian fluid in a rotating frame of reference is

$$\frac{\partial \mathbf{u}}{\partial t} + (\mathbf{u}\cdot\nabla)\mathbf{u} + 2\mathbf{\Omega} \times \mathbf{u} = -\frac{1}{\rho}\nabla p - |\Omega|^2 \mathbf{r}_\perp + \nu\Delta\mathbf{u} \tag{1}$$

where $\mathbf{u}$ is the velocity vector, Ω the rotation vector of the system, ρ the fluid density, p the pressure, $\mathbf{r}_\perp$ the distance from the axis rotation axis, and ν the fluid's kinematic viscosity, e.g. [5].

In the absence of rotation, the balance of inertial to viscous terms is quantified by the Reynolds number when typical scales U_0 and L are used to scale the velocities and length scales, respectively:

$$\frac{(\mathbf{u}\cdot\nabla)\mathbf{u}}{\nu\Delta\mathbf{u}} \longrightarrow \frac{U_0^2/L}{\nu U_0/L^2} \longrightarrow Re \equiv \frac{U_0 L}{\nu}. \tag{2}$$

The standard developing laminar boundary layer over a flat plate is the Blasius layer, e.g. [1] with a thickness δ given by

$$\frac{\delta}{x} = \frac{5}{\sqrt{Re_x}}, \tag{3}$$

where x is the stream wise distance from the leading edge and $Re_x = U_0 x/\nu$ the local Reynolds number using that distance as the length scale.

In a rapidly rotating fluid, the Coriolis term becomes a major term in the force balance, and the momentum equations can be scaled by that term, so that the ratio of the viscous term to the Coriolis term becomes

$$\frac{\nu\Delta\mathbf{u}}{2\mathbf{\Omega} \times \mathbf{u}} \longrightarrow \frac{\nu U_0/L^2}{2\Omega U_0} \longrightarrow E \equiv \frac{\nu}{\Omega L^2}. \tag{4}$$

The relative magnitude of the centrifugal and Coriolis terms are given by

$$\frac{|\Omega|^2 \mathbf{r}_\perp}{2\mathbf{\Omega} \times \mathbf{u}} \longrightarrow \frac{\Omega^2 R}{2\Omega U_0} \longrightarrow \lambda \equiv \frac{\Omega R}{U_0}. \tag{5}$$

Since this nondimensional has the same form as the tip speed ratio, well known for wind turbines, it is referred to here as the speed ratio where the factor 2 has been dropped to maintain similarity to the tip speed ratio.

The presence of the Coriolis terms leads to the boundary layer in a rotating fluid if there is relative motion of the fluid to a boundary [5]. On a horizontal boundary and a vertical axis of rotation, this boundary layer equilibrates to an Ekman boundary layer of thickness

$$\delta_E = \sqrt{\frac{\nu}{\Omega}} \tag{6}$$

with a velocity profile of

$$u_E = U_0 \left(1 - e^{-z/\delta_E} \cos(z/\delta_E)\right) \tag{7}$$

$$v_E = U_0 \quad e^{-z/\delta_E} \sin(z/\delta_E) \tag{8}$$

The Blasius profile and the two components of the flow in the basic Ekman layer are shown in Figure 1, where the vertical axis has been scaled against the Ekman layer thickness, and the boundary layer thickness of the Blasius layer was set to 2.5δ. It can be seen that there is substantial crossflow in the Ekman layer at a height of around δ_E and that the flow overshoots slightly before reaching the freestream velocity. To maintain mass continuity, a consequence of this Ekman layer is that a vertical velocity is induced at the top of the boundary layer, known as Ekman pumping, of

$$w_E = \frac{\sqrt{E}}{2}\zeta_0, \tag{9}$$

where $\zeta_0 = (\partial v_0/\partial x - \partial u_0/\partial y)$ is the vorticity of the flow at the top of the Ekman layer.

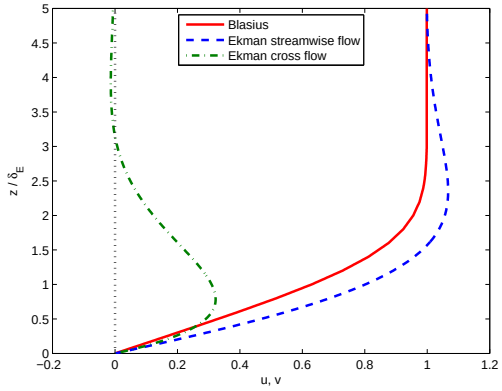

Figure 1: Velocity profiles for the Blasius layer (solid line), and the Ekman layer (dashed line for the streamwise velocity and dash-dotted line for the crossflow velocity.

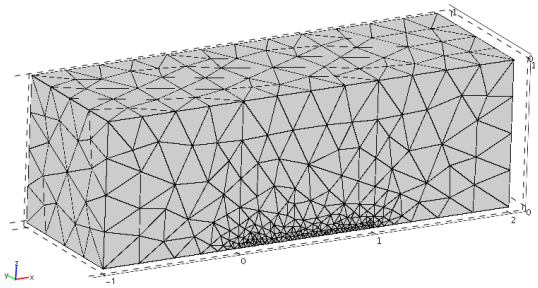

Figure 2: The domain and mesh for the simulation of the effect of the rotor's rotation.

For a section on a typical wind turbine blade, of say a chord of 1m at a distance of 30m from the axis, rotating at 20rpm, in a wind of 12m/s, the three nondimensional parameters are of the order of $Re \sim 10^6 - 10^7$, $E \sim 10^{-5}$, and $\lambda \sim 5$, and typical boundary layer thicknesses are δ 10^{-2}m and δ_E $10^{-3} - 10^{-2}$m. This suggests that the Ekman layer may play a significant role in the development of the boundary layer on the turbine blade.

2 Model and Methodology

To investigate the process by which the rotation rate of the rotor may affect the development of the boundary layer, a very simple model was devised: the development of viscous flow over a flat plate section under the influence of Coriolis and centrifugal effects was simulated in a 3D Finite-Element code using *COMSOL*. The domain consisted of three cuboid subdomains, all with an edge length of 1, as indicated in figure 2. The first had a face with inlet velcocity conditions of $u = U_0, v = w = 0$ and a stress-free lower boundary, the central subdomain had no-slip condition at the lower boundary, while the last subdomain had again a stress-free lower boundary as well as outflow conditions ($p = 0$). To resolve the boundary layer appropriately, the mesh resolution was highest at the lower boundary in the middle section, with a largest linear element size of 0.1, 0.05, and 0.025 to test the model for sensitivity to the resolution.

The initial solution was a stationary solution obtained at $\rho = 1$, $\nu = 0.1$, $U_0 = 10$, $\Omega = 2$, and

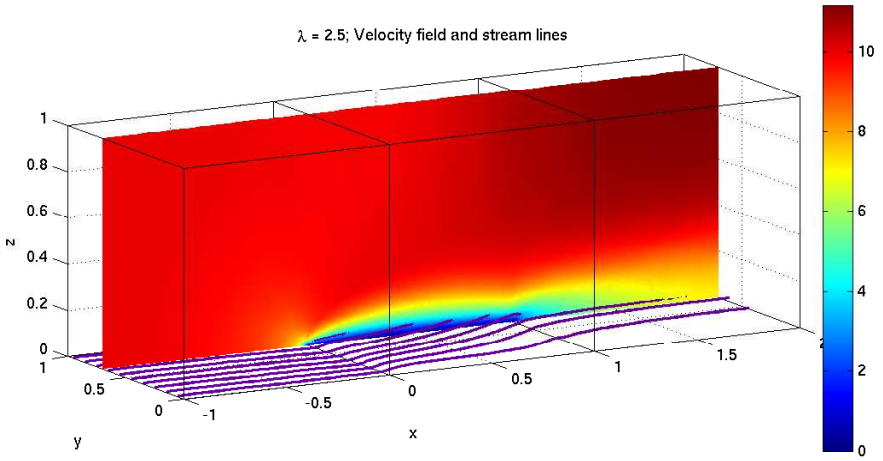

Figure 3: A typical solution at $\Omega = 5$, $Re = 100$, $E = 0.02$, and $\lambda = 2.5$. Shown is a vertical slice of the velocity magnitude, $|u| = (u^2 + v^2 + w^2)^{1/2}$, and a set of stream lines originating in a plane at height $z = 0.02$.

$R = 5$. This set of parameters leads to nondimensional parameters of $Re = 100$, $E = 0.05$, and $\lambda = 1$. From this, three sets of stationary solutions were obtained using the stationary parametric solver of *COMSOL*,

1. changing the viscosity: $\nu = 0.02 - 1.0$ – this affects the Reynolds and Ekman numbers;
2. changing the rotation rate: $\Omega = 1 - 10$ – this affects the Ekman number and Speed ratio;
3. changing the radius: $R = 5 - 100$ – this only affects the speed ratio

While it was initially planned to cover larger ranges of viscosity and rotation rate, this was not possible with the computing resources available since the required mesh for reliable results exceeded the available memory.

Since only one parameter was changed at a time, all parameter values not explicitly given in Section 3 are those from the initial solution.

3 Results

Figure 3 shows a representative solution at $\Omega = 5$. The onset of the developing boundary layer is clearly seen in the colour/shading of the slice showing the magnitude of the velocity field. One can also see that the growth of the boundary layer as indicated by the velocity magnitude appears to be limited from about half-way along the plate. At the same time, the streamlines demonstrate the cross-flow induced by the rotation of the plate. This generic structure was seen for all results obtained. From the three-dimensional velocity field, vertical profiles of the three velocity components were extracted. A boundary layer thickness was estimated at the thickness at which the profile of the stream wise velocity, $u(z)$, reached 99% of the maximum within that profile.

Figure 4 shows velocity profiles for different values of the viscosity. As this affects both the Reynolds number and the Ekman number, one can see two effects; Figure 4(a) shows how the boundary layer thickness reduces as the the effective Reynolds number increases from $Re = 10$ at $\nu = 1$ to $Re = 500$ at $\nu = 0.02$. Also, the crossflow becomes concentrated into the reduced boundary layer and the velocity maximum increases from $v \sim 0.05$ at $\nu = 1$ $(E = 0.5)$ to $v \sim 0.2$ at $\nu = 0.02$ $(E = 0.01)$.

(a)

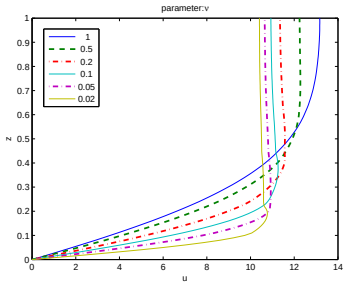

(b)

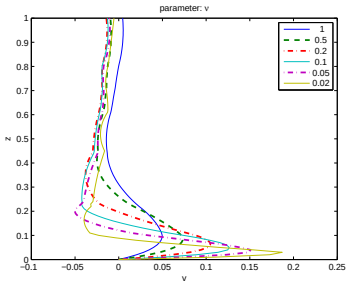

Figure 4: Vertical profiles in the centre of the flat plate of the streamwise velocity in (a) and crossflow velocity in (b) where the parameter for the different lines is the viscosity.

(a)

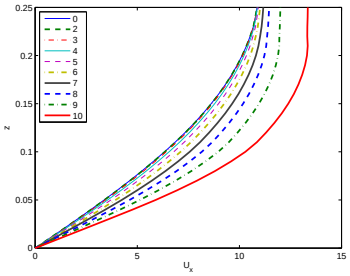

(b)

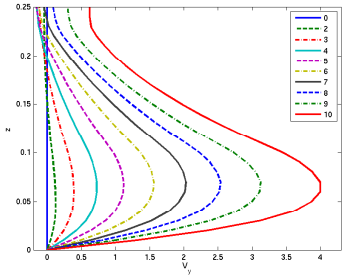

Figure 5: Vertical profiles in the centre of the flat plate of the streamwise velocity in (a) and the crossflow velocity in (b) where the parameter for the different lines is the rotation rate.

(a) (b)

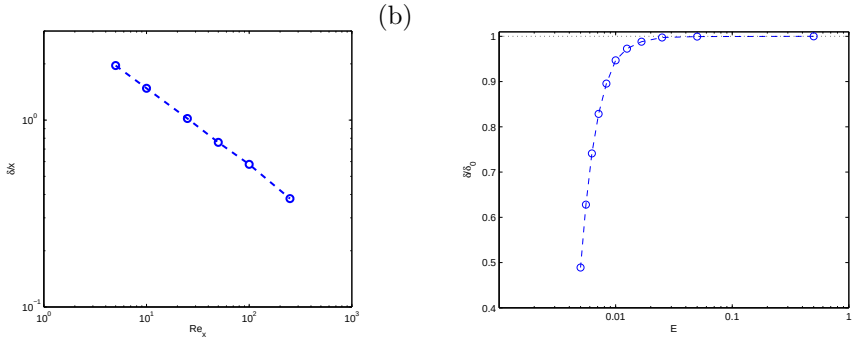

Figure 6: An estimate of the boundary layer thickness in the centre of the flat plate against (a) the Reynolds number and (b) the Ekman number.

Figure 5 shows the corresponding results for different values of the rotation rate. The Reynolds number is constant, $Re = 100$, but the Ekman number decreases from $E = 0.5$ to $E = 0.01$, covering the same range as that covered by changing the viscosity. Here, the reduction of the boundary layer thickness, as estimated from is much less than where both nondimensional parameters are changed. The effect on the crossflow, however, is substantial, reaching a peak cross flow velocity of $v \sim 4$ at $E = 0.01$, compared to $v \sim 0.2$ also at $E = 0.01$ but $Re = 500$. Finally, changing the speed ratio only but keeping both the Ekman number and the Reynolds number constant, leads to a situation, where the boundary layer thickness is virtually constant but the behaviour of crossflow velocity is very similar to that shown in Figure 5(b)

The variation of the boundary layer thickness against the two main dimensional parameters is summarised in Figure 6. Figure 6(a) shows the ratio of the boundary layer thickness to the distance from the leading edge, δ/x, against the local Reynolds number where the viscosity was changed, while Figure 6(b) shows the boundary layer thickness normalised by that at zero rotation rate where the rotation rate was changed agains the Ekman number. Quite clearly, the boundary layer thickness reduces as the Reynolds numer increases, and it also reduces as the Ekman number decreases. The variation of the thickness against the Reynolds number is well correlated to a curve of the shape $\delta/x = 3.88Re^{-0.42}$ $(r^2 > 0.999)$. The dependency of the thickness with respect to the Ekman number is less easy to quantify but it appears that the boundary layer thickness is modified to only a minor extend as long as the Ekman number is above a certain value but then changes rapidly below that value.

4 Conclusions

We have presented results from a set of parametric studies of the developing laminar boundary layer over a flat plate subjected to the additional Coriolis and centrifugal forcing terms arising from the rotation of the plate around an axis perpendicular to the plate's surface.

The velocity structure in the boundary layer is similar to that of a combination of the Blasius and Ekman layers, with a stream wise velocity approaching the freestream velocity with distance from the plate but also with a substantial crossflow roughly in the centre of the boundary layer. The scaling of the boundary layer thickness is affected by the rotation rate to a degree where the thickness is reduced, and the scaling with the Reynolds number deviates from the standard scaling of $\sim Re^{-0.5}$; the case presented here showed a scaling of $\sim Re^{-0.42}$ instead. It was found that the centrifugal term, as measured by the Speed ratio, did not affect the boundary layer thickness but the magnitude of the crossflow velocity, whereas the Coriolis term appears to affect the boundary layer thickness. Figure 6 indicated a rapid reduction in the boundary layer thickness below a certain Ekman number. Returning to the basic boundary layers the thickness is overlaid with the basic theoretical values for the Blasius layer and the Ekman layer, respectively, in Figure 7. This suggests that effect of the rotation on the

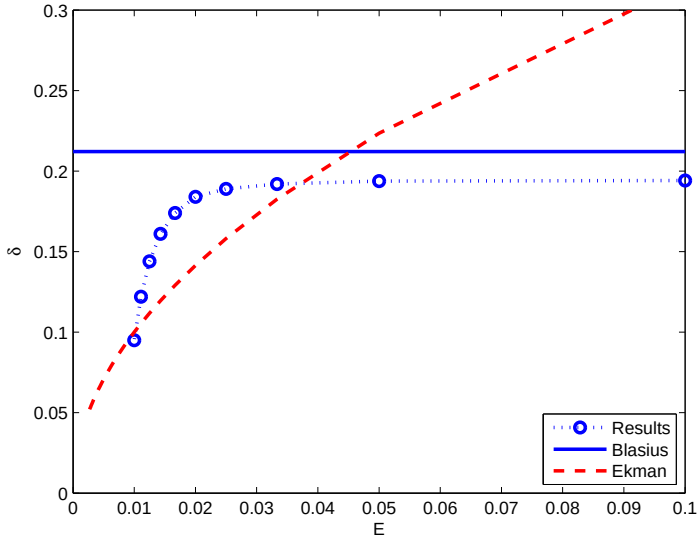

Figure 7: Comparison of the measured boundary layer thickness (circles and dotted line), the Blasius boundary layer (solid line), and the Ekman thickness (dashed line) against Ekman number.

boundary layer thickness sets in at a point where the Ekman thickness is about half the Blasius layer thickness and then rapidly limits the boundary layer towards that of the Ekman layer. This factor of about half is also represented in Figure 1, where the Blasius boundary layer was taken to have a thickness of $2.5\delta_E$.

The second effect of the rotation is also the an induced suction at the top of the boundary layer, which is strongly affected by the Coriolis and centrifugal terms, as found by changing both the Ekman number and Speed ratio together, and by changing the Speed ratio alone.

These two effects can work together to reduce the effect of an adverse pressure gradient. The limiting of the boundary layer thickness means that a smaller portion of the fluid is susceptible to stagnation, and the Ekman suction will introduce fluid with higher momentum into the boundary layer. While the analysis was at present only completed for laminar flow at low Reynolds numbers, the effects of induced cross flow and Ekman suction should persist for turbulent flows as well.

Acknowledgments

The author wishes to thank the Royal Academy of Engineering who supported this work through a Global Research Award and an International Travel Grant.

References

[1] B.R. Munson and D.F. Young and T.H. Okiishi. *Fundamentals of Fluid Mechanics*. Wiley, New York, 2nd edition, 1994.

[2] E. M. Smirnov and A. V. Shatrov. Development of the boundary layer on a plate in a rotating system. *Fluid Dynamics*, 17(3):452 – 455, 1982.

[3] H. Snel. Scaling laws for the boundary layer flow on rotating wind turbine blades. In K.F. McAnulty, editor, *4th IEA Symposium on Aerodynamics for Wind Turbines*, ETSU-N-118, Rome, 1991.

[4] J. G. Leishman. Challenges in modelling the unsteady aerodynamics of wind turbines. *Wind Energy*, 5:85–132, 2002.

[5] J. Pedlosky. *Geophysical Fluid Dynamics*. Springer-Verlag, Berlin, Heidelberg, New York, second edition, 1987.

[6] S.J. Schreck and N.N. Sørensen and M.C. Robinson. Aerodynamic structures and processes in rotationally augmented flow fields. *Wind Energy*, 10:159 – 178, 2007.

[7] W. Banks and G. Gadd. Delaying effect of rotation on laminar separation. *AIAA Journal*, 1:941 – 942, 1963.